journal

J. Am. Ceram. Soc., **85** [9] 2325–30 (2002)

Inhibition of Sintering and Surface Area Loss in Phosphorus-Doped Corundum Derived from Diaspore

Richard L. Smith*,† and Svetlana V. Yanina

Department of Materials Science and Engineering, Massachusetts Institute of Technology, Cambridge, Massachusetts 02139

Gregory S. Rohrer*

Department of Materials Science and Engineering, Carnegie Mellon University, Pittsburgh, Pennsylvania 15213

Anthony J. Perrotta*,**

Materials Research Laboratory, Pennsylvania State University, State College, Pennsylvania 16802

The influence of magnesium, phosphorus, and iron additions on the low-temperature (≤1000°C) sintering of nanocrystalline α-Al_2O_3 derived from α-AlOOH has been investigated. α-AlOOH powder with a surface area of 50 m^2/g yielded α-Al_2O_3 products with surface areas of 150 and 80 m^2/g after dehydration at temperatures of 400° and 500°C, respectively. However, these products were prone to sintering at >600°C, and the surface area was reduced to 15 m^2/g within only 1 h at 1000°C. Although magnesium and iron doping had no discernible effect, the presence of phosphorus inhibited sintering and surface-area loss significantly. Samples doped with 1%–2% phosphorus had surface areas of >31 m^2/g after 100 h at 1000°C. Atomic force microscopy studies of α-Al_2O_3 pseudomorphs derived from α-AlOOH single crystals also demonstrated the inhibiting effect of phosphorus, as the rate of crack elimination was reduced on phosphorus-modified surfaces. The effects of the dopants are discussed with regard to their potential influence on α-Al_2O_3 surface energy and diffusivity.

I. Introduction

TRANSITION aluminas, such as γ-Al_2O_3, are readily synthesized in nanoparticulate forms with surface areas of >100 m^2/g.[1–5] These metastable phases resist coarsening and sintering at temperatures up to ~900°C, which has contributed to their widespread application as adsorbents and heterogeneous catalyst supports.[6] Through the incorporation of dopants that inhibit their transformation to corundum (α-Al_2O_3), their ranges of stability and use can be extended up to almost 1200°C, although typically at surface areas of <70 m^2/g.[7–12] Although transition aluminas are well-suited for many applications, experimental results have indicated that α-Al_2O_3 could be superior in certain cases, if it could be prepared in a comparable nanocrystalline form. For example, rhodium, which is an active component in three-way automotive emissions catalysts, maintains catalytic activity up to 900°C when supported on α-Al_2O_3, whereas γ-Al_2O_3-supported rhodium begins to lose activity at >650°C.[13] Similarly, MoS_2-based hydrodesulfurization catalysts supported on α-Al_2O_3 have been reported to exhibit higher specific activities than those supported on γ-Al_2O_3.[14]

In contrast to the transition aluminas, nanocrystalline α-Al_2O_3 traditionally has been difficult to synthesize. An established route is through the dehydration of diaspore (α-AlOOH), which is a natural constituent of some bauxites and can be synthesized hydrothermally.[1–5] α-AlOOH decomposes topotactically (pseudomorphically) to α-Al_2O_3 at ~400°C and, under appropriate conditions, yields nanocrystalline products with surface areas of >150 m^2/g.[15–20] Over the past year, two new routes to nanocrystalline α-Al_2O_3 have been identified.[21,22] An exciting aspect of these processes is that they use precursors that are both synthesized and transformed to α-Al_2O_3 at ambient pressure. Hence, they circumvent the principle difficulty associated with synthesis from α-AlOOH and may well offer additional advantages. A major obstacle to support and adsorbent applications still exists however, because nanocrystalline α-Al_2O_3 is prone to rapid sintering and surface-area loss between 500°C and 1000°C, temperatures where γ-Al_2O_3 and the other transition aluminas resist coarsening.[6,18]

Recent microcalorimetry measurements have evaluated the anhydrous surface energies of α-Al_2O_3 and γ-Al_2O_3 as being 2.7 and 1.7 J/m^2, respectively.[18,19] This observation might, in part, account for the disparate low-temperature-sintering behavior of these phases; however, differences in their transport characteristics probably also make a contribution. Water (H_2O) chemisorption (surface hydroxylation) reduces the surface energies of both polymorphs but has a greater effect on α-Al_2O_3, because equilibrated α- and γ-Al_2O_3 powders exhibit virtually equivalent ambient hydroxyl coverages (~17 OH molecules per square nanometer) and surface energies.[18,19] However, at 500°–900°C, α-Al_2O_3 maintains an almost-constant hydroxyl coverage (~9 OH molecules per square nanometer) that is 2–3 times greater than that of γ-Al_2O_3.[19] This difference is significant because, along with enhancing hydroxylation, H_2O vapor accelerates a number of low-temperature processes in aluminas that are likely controlled by surface diffusion, including the growth of α-Al_2O_3 nuclei in transition alumina beds,[23–25] transition alumina coarsening,[5,10,25] and surface-area loss in nanocrystalline α-Al_2O_3 that has been derived from α-AlOOH.[26] Because hydroxylation should reduce the driving force (i.e., surface energy) for at least the latter two processes, it must also enhance the transport kinetics. Hence, the susceptibility of α-Al_2O_3 to hydroxylation may establish conditions where the accompanying reduction in surface energy is offset by a disproportionate increase in diffusivity.

J. Blendell—contributing editor

Manuscript No. 187171. Received February 5, 2002; approved May 22, 2002.
Supported in part by the Aluminum Company of America and the National Science Foundation, under YIA Grant DMR-9458005, and by the Dept. of Materials Science and Engineering of the Massachusetts Institute of Technology.

*Member, American Ceramic Society.
**Fellow, American Ceramic Society.
†Author to whom correspondence should be addressed.

Prior studies have shown that dopants and impurities can have significant effects on the coarsening of transition aluminas and their conversion to α-Al_2O_3,[3,7–12] as well as sintering and microstructure development in bulk α-Al_2O_3.[27–29] Although the mechanisms underlying such effects are often subject to debate, dopants have the potential to impact both the thermodynamic (e.g., interfacial energies) and kinetic factors (e.g., diffusivities and boundary mobilities) that are pertinent to the respective processes.[28,29] The objective of this study was to investigate the feasibility of using surface dopants/modifiers to inhibit low-temperature ($\leq$1000°C) sintering and surface-area loss in nanocrystalline α-Al_2O_3 derived from α-AlOOH. Little has been reported on the influence of dopants on α-Al_2O_3 sintering at temperatures below ~1400°C. Therefore, several modifiers (magnesium, phosphorus, and iron) that have been shown to have rather different effects on the coarsening of transition aluminas and their conversion to α-Al_2O_3 has been investigated. Phosphorus inhibits both processes, whereas magnesium and iron generally either moderately enhance them or have no effect.[3,7–12,27,30] Although the mechanisms by which the dopants modify coarsening and conversion behavior are not well understood, both processes require long-range diffusion. Thus, the kinetics of transport, as well as the driving force, could potentially be altered.[7,23] The influence of the dopants on α-Al_2O_3 sintering has been examined through specific surface area measurements and atomic force microscopy (AFM) studies of samples that were derived from α-AlOOH powders and single crystals, respectively. Phosphorus inhibits sintering and surface-area loss, whereas magnesium and iron have no discernible effect. Hence, the dopants have similar effects in both transition aluminas and α-Al_2O_3.

II. Experimental Procedure

(1) Powder Preparation, Sintering, and Characterization

Coarse α-AlOOH powder was synthesized hydrothermally and then dry-milled to a surface area of 50 m^2/g using α-Al_2O_3 media.[17] Previous microscopic observations have shown that such powders are comprised of platy, (010)-oriented particles that can be reasonably modeled as square plates of edge length l and thickness d, having an aspect ratio m of ~3 ($m = l/d$).[20] Based on this model, an average α-AlOOH particle size (~l) on the order of 60 nm would be expected for the 50 m^2/g powder. Even allowing for the possibility that m could vary over a range of 2–6, comparable particle sizes of 48–93 nm would still be expected. Magnesium, phosphorus, and iron were incorporated onto the α-AlOOH powders as salts using a solution impregnation approach. Aqueous solutions were prepared using $Mg(NO_3)_2 \cdot 6H_2O$ (ACS reagent, Fisher Scientific, Pittsburgh, PA), H_3PO_4 (85%, Alfa Aesar, Danvers, MA), $Fe(NO_3)_3 \cdot 9H_2O$ (ACS reagent, Alfa Aesar), and deionized H_2O. In a typical synthesis, 0.3 g of α-AlOOH was suspended in 15 mL of solution with a concentration appropriate for the desired doping level. Bulk dopant concentrations of 0.1–5 at.% (metals basis) were examined, corresponding to α-AlOOH surface loadings of ~0.2–10 dopant atoms (Mg, P, or Fe) per square nanometer. After stirring for 2 h at room temperature, the sols were dehydrated by heating (~90°C) under constant stirring. The impregnated powders were then loaded into α-Al_2O_3 crucibles and calcined in static air at ambient humidity in a muffle furnace. The powders were annealed in two stages. The first was a 6 h soak at moderate temperature (400° or 500°C) to cause decomposition of the salts and α-AlOOH. The temperature was then increased at a rate of 5°C/min to the desired sintering temperature (up to 1000°C), where the samples were held for a predetermined period of time.

The specific surface areas of the calcined products were characterized by nitrogen absorption, using the multipoint Brunauer–Emmett–Teller (BET) method (Model NOVA 1000, Quantachrome Instruments, Boynton Beach, FL). Before measurement, the samples were outgassed for 3 h at 250°C under vacuum. Repeated trials of several samples, which had surface areas of 10–40 m^2/g, over the course of study demonstrated day-to-day and measurement-to-measurement variability of less than $\pm$1 m^2/g. The surface areas reported in Section III have been rounded to the nearest 1 m^2/g to reflect this variability. Powder X-ray diffraction (XRD) was used to assess the phase composition of select products. Samples were analyzed using a θ–θ diffractometer (Rigaku, Tokyo, Japan) with Cu$K\alpha$ radiation supplied by a rotating-anode generator that was operated at 60 kV and 300 mA.

(2) Single-Crystal Atomic Force Microscopy Studies

Atomic force microscopy (AFM) was used to characterize the effects of various thermal and doping treatments on the morphology and pore structure of α-Al_2O_3 pseudomorphs derived from α-AlOOH single crystals. Natural specimens of α-AlOOH were supplied by the National Museum of Natural History of the Smithsonian Institution in Washington, DC (Smithsonian catalog number 81900-1). The specimens were originally collected in Chester, MA. The crystals were characteristically platy (~3 mm × 4 mm × 1 mm) with large {010} faces and had optical appearances ranging from colorless and transparent to translucent and gray. Only colorless specimens were used. Following the doping (described below) and thermal treatments, the former {010} surfaces of the calcined α-AlOOH crystals, now α-Al_2O_3 pseudomorphs, were characterized using AFM (Model Nanoscope E, Digital Instruments, Santa Barbara, CA) in an argon-filled glove box with H_2O and oxygen-gas (O_2) levels of <5 ppm. Observations were made in the contact mode using pyramidal silicon nitride (Si_3N_4) cantilevered tips and load forces of 0.1–8 nN.

The α-AlOOH(010) surface and its pseudomorphic α-Al_2O_3 decomposition product were the focus of study for several reasons. α-AlOOH powder particles are characteristically platy with large {010} faces. Hence, {010} surfaces are expected to comprise a large fraction—in excess of 60% for $m \geq 3$—of the total surface area of α-AlOOH powder samples and, correspondingly, of their α-Al_2O_3 decomposition products.[20] Furthermore, fresh {010} surfaces for study are readily formed by cleavage with a razor blade. The single-crystal surfaces were "doped" by dipping them into a dopant solution of known concentration to attain a thin surface film, which was then allowed to dry at 120°C. Single crystals were first cleaved in half normal to the [010] axis to form pairs of crystals with mated {010} surfaces. Then, one crystal from each mated pair was doped, while the other was left undoped, so it could be used as a control sample for comparison.[31] Then, the doped and control surfaces were subjected to the same heat treatment. Typically, two or three areas on three or four mated pairs of surfaces were examined, to ensure that the observations were characteristic and not the result of spurious impurities in any particular crystals or crystal regions. Similar mating approaches were also used to compare the effects of different thermal treatments. Noticeable differences in the behaviors of α-AlOOH{010} surfaces, mated or not, that had been treated under identical conditions were not observed.

III. Results

(1) Sintering of α-Al_2O_3 Derived from α-AlOOH

The 50 m^2/g α-AlOOH powder yielded α-Al_2O_3 products with surface areas on the order of 150 and 80 m^2/g when it was calcined for 6 h at 400° and 500°C, respectively. Subsequent anneals at higher temperatures resulted in substantial reductions in surface area. For example, after treatment for 6 h at 500°C and then 1 h at 700°C, the surface area was reduced to 33 m^2/g. If the α-Al_2O_3 was instead held for 1 h at 1000°C, the measured surface area was only 15 m^2/g. After 24 h at 1000°C, the surface area was decreased to 11 m^2/g. Although the surface areas of products calcined at 400° and 500°C were initially much different, their surface areas differed by less than the uncertainty of the measurement ($\pm$1 m^2/g) after subsequent anneals of >1 h at 1000°C.

The {010} cleavage surfaces of α-AlOOH single crystals were characterized by atomically flat terraces that were separated by steps that were an integer multiple of $b/2$ (0.47 nm) (see Fig. 1(a)). Following decomposition, the α-Al_2O_3 pseudomorph surfaces were marked by arrays of pore channels or cracks that were

oriented along the [100] and [001] axes of the parent α-AlOOH crystals (see Figs. 1(b) and (c)), which is consistent with previous optical microscopy observations.[16] Based on the well-known topotactic relationship between α-AlOOH and α-Al_2O_3, the pseudomorphs are comprised of assemblages of α-Al_2O_3 crystallites with their [0001], [11$\bar{2}$0], and [1$\bar{1}$00] axes parallel to the parent [100], [010], and [001] axes.[15,16] The most conspicuous difference between surfaces decomposed at 400° (Fig. 1(b)) and 500°C (Fig. 1(c)) was that the former had a higher density of cracks. These defects presumably formed to relieve stress as water evolved from the crystals during dehydration. Comparable cracks were probably absent from the powders, because the distances between adjacent cracks on pseudomorph surfaces were always greater than the average particle size (50–100 nm) of the α-AlOOH powder. Although they were not resolved in AFM images, nanometer-scale pores have previously been observed in transmission electron microscopy (TEM) studies of α-Al_2O_3 derived from particulate α-AlOOH.[32] The reduced surface area of powders calcined at 500°C was presumably due to coarsening of these nanopores.[32,33]

Under the idealized assumptions that each α-AlOOH powder particle ultimately yields one fully dense α-Al_2O_3 pseudomorph and inter-pseudomorph sintering (i.e., the formation and growth of necks between pseudomorphs) does not occur, one would expect 50 m^2/g α-AlOOH to yield α-Al_2O_3 with a surface area of 48 m^2/g. This value is based simply on the surface area of the parent powder and the respective molecular weights (59.99 and 101.96 g/mol) and densities (3.44 and 3.98 g/cm^3) of α-AlOOH and α-Al_2O_3. It is independent of the morphology of the parent particles, as long as the product maintains this morphology. α-Al_2O_3 that has been derived from α-AlOOH at 400°–500°C is porous at the nanometer scale.[32] Therefore, it is not surprising that the products had initial surface areas well in excess of the idealized 48 m^2/g. However, after 1 h at >700°C, the surface areas were appreciably less than this value. Therefore, in addition to pore coarsening and elimination within individual pseudomorphs, the loss of surface area must also involve inter-pseudomorph sintering and/or changes in pseudomorph morphology that reduce their surface-to-volume ratio. Although a change in pseudomorph morphology cannot be excluded, simple geometric calculations show that this factor alone could not account for the large decreases in surface area at >700°C, because surface areas of 37–27 m^2/g would be expected, even if the ideal platy pseudomorphs ($m \approx$ 2–6) were to evolve into the form of spheres during annealing.

(2) Influence of Magnesium, Phosphorus, and Iron Additions on the Sintering of α-Al_2O_3

α-AlOOH precursor powders with magnesium, phosphorus, and iron loadings of 0.1% and 1% were prepared by solution impregnation and subsequently calcined for 6 h at 500°C and 24 h at 1000°C. The surface areas of the resulting magnesium- and iron-doped α-Al_2O_3 products were all within ±1 m^2/g of that of an undoped sample (11 m^2/g) that had been treated under identical conditions. On the other hand, additions of 0.1% and 1% phosphorus resulted in appreciably greater α-Al_2O_3 surface areas (16 and 34 m^2/g, respectively). The surface areas of doped and undoped products were all 80 ± 4 m^2/g after the initial dehydrating treatment (500°C). The time-dependent evolution of the surface areas of undoped and 1%-phosphorus-doped samples during anneals at 1000°C is presented in Fig. 2. After 1 h, the surface areas of the undoped and phosphorus-doped α-Al_2O_3 had been reduced from ~80 m^2/g to 15 and 45 m^2/g, respectively. After 100 h, the undoped and phosphorus-doped products had respective surface areas of 10 and 32 m^2/g. Similar trends were observed at 900°C. After 50 h, the 1%-phosphorus-doped α-Al_2O_3 had a surface area of 43 m^2/g, whereas the undoped samples and those samples that had been doped with 1% magnesium and 1% iron had coarsened to <14 m^2/g.

Because significant differences were observed between the surface areas of samples doped at 0.1 and 1% phosphorus, additional concentrations were investigated. Series of α-AlOOH

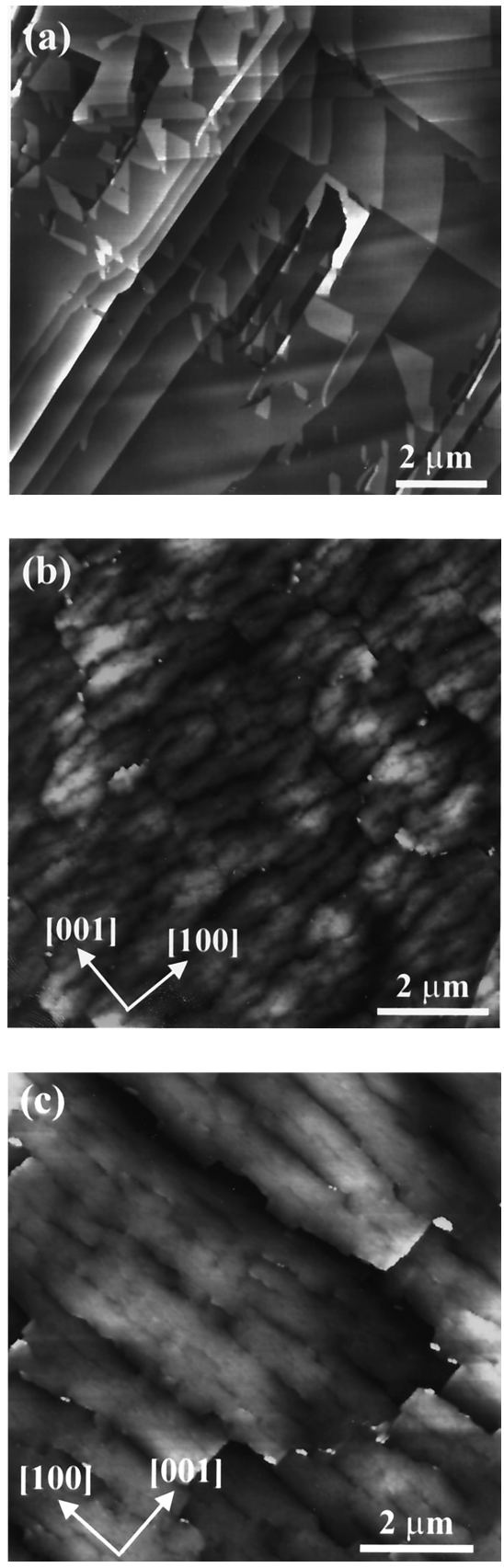

Fig. 1. Topographic AFM images of (a) a freshly cleaved α-AlOOH(010) surface, (b) an α-AlOOH(010) surface (now an α-Al_2O_3 pseudomorph) after a 12 h anneal at 400°C in air, and (c) an α-AlOOH(010) surface after a 12 h anneal at 500°C in air. The black-to-white contrast in Figs. 1(a), (b), and (c) corresponds to topographic ranges of 7, 100, and 90 nm, respectively. The crystallographic directions in Figs. 1(b) and (c) are shown with respect to the parent α-AlOOH crystals.

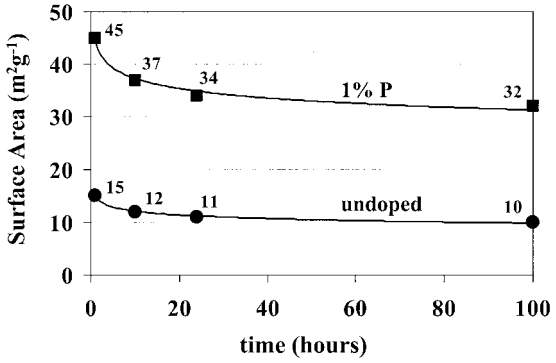

Fig. 2. Specific surface areas of undoped and 1% phosphorus-doped α-Al_2O_3 products plotted versus annealing time (t = 1, 12, 24, and 100 h) at 1000°C. The α-AlOOH precursors were dehydrated at 500°C (for 6 h) before annealing at 1000°C. The surface areas of the undoped and phosphorus-doped products each were 80 ± 4 m^2/g after the initial dehydrating treatment (at 500°C). Curves are intended solely to guide the eye.

precursors with phosphorus loadings up to 5%, at 1% intervals, were prepared using phosphoric acid (H_3PO_4). The powders were then treated for 6 h at 400°C and 24 h at 1000°C. The surface areas of the products are presented in Fig. 3. A maximum of 36 m^2/g was observed at a phosphorus loading of 2%. Additional trials were also conducted with 2 and 5% magnesium and iron; however, no differences (±1 m^2/g) were observed between the surface areas of doped and undoped samples after 24 h at 1000°C. XRD analysis revealed that products that had been doped with 4%–5% phosphorus contained small amounts of aluminum phosphate ($AlPO_4$) (cristobalite type). Because the phase-detection limit of XRD is ~5%–10%, the formation of aluminum phosphates at the lower concentrations cannot be excluded. Using the specific surface areas and bulk doping levels of the calcined products, upper limits can be placed on the average phosphorus concentrations at their surfaces. This procedure requires the assumptions that all the phosphorus resides at external surfaces (those probed by the surface-area measurement) and that there are no losses (for example, due to solid solubility, evaporation, or $AlPO_4$ precipitation). For the samples that have been doped with 1% and 2% phosphorus, which had corresponding surface areas of 31 and 36 m^2/g, the average surface concentrations had to be less than or equal to 4 and 7 P atoms per square nanometer, respectively. For comparison, the average surface site densities of Al and O, calculated based on the bulk density and molecular weight of α-Al_2O_3, are ~13 Al and 17 O atoms per square nanometer.

One concern with the phosphorus doping procedure was that some portion of the α-AlOOH powder might dissolve in the acidic

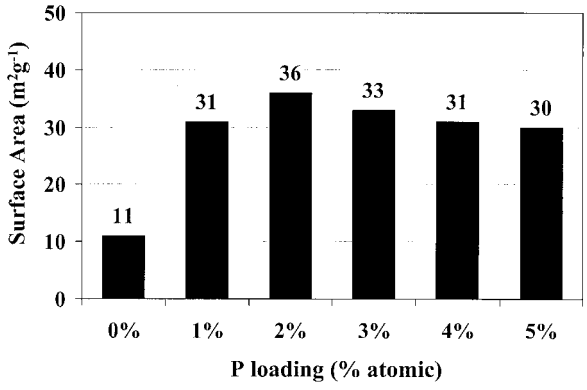

Fig. 3. Variation of the specific surface areas of α-Al_2O_3 powders relative to the level of phosphorus doping (atomic percent) after 24 h at 1000°C. The α-AlOOH precursors were dehydrated at 400°C (for 6 h) before annealing at 1000°C.

H_3PO_4 solutions (initial pH ~2.1 for 2% phosphorus). Any material dissolved was expected to precipitate as other aluminum hydroxides, most likely boehmite, as the sols were dried. When calcined, these hydroxides would yield transitions aluminas, which resist coarsening and conversion to α-Al_2O_3 when doped with phosphorus.[10,12] Although transition phases were never detected via XRD in the products, it seemed reasonable to investigate a less-aggressive doping solution. Precursors with 1%–5% phosphorus were prepared in 1% increments using ammonium phosphate ($(NH_4)_2HPO_4$, ACS reagent, Fisher Scientific), which is a mildly basic salt, in place of H_3PO_4. The precursors were then treated for 6 h at 400°C and 24 h at 1000°C. The specific surface areas of these products did not differ from their counterparts that had been doped with H_3PO_4 (Fig. 3) by more than ±1 m^2/g. Hence, solution–precipitation phenomena during doping had little effect on the final surface areas of the products. This finding could also be inferred from the fact that the surface area decreased as the phosphorus loading increased (Fig. 3), because α-AlOOH solubility and, thus, the potential for transition alumina formation should have been enhanced by the increasingly acidic H_3PO_4 doping solutions.

AFM experiments with α-AlOOH single crystals demonstrated that the presence of phosphorus slowed the rate of crack/pore elimination on α-Al_2O_3 pseudomorph surfaces. AFM images of doped and undoped surfaces following a treatment of 12 h at 400°C and 10 h at 1000°C are presented in Fig. 4. The doped precursor (α-AlOOH) surface was dip-coated with a 0.1*M* H_3PO_4 solution before the anneal. Through treatments of >24 h, phosphorus-doped surfaces maintained a noticeable fraction of the cracks introduced during decomposition (see Fig. 4(a)), whereas few cracks persisted on undoped surfaces treated for >6 h (see Fig. 4(b)). Most regions were smooth and featureless over areas of >10 μm^2, which indicated that many cracks had healed perfectly. When cracks did not heal perfectly, grain boundaries were left behind, most frequently along the [100] axis of the parent α-AlOOH crystal. The phosphorus concentrations on doped pseudomorph surfaces were difficult to quantify, because the thickness of the liquid doping films could not be measured directly. Because the H_3PO_4 solutions wetted the α-AlOOH(010) surface, it is reasonable to assume that the films were <100 nm thick. Considering values between 10 and 100 nm, the phosphorus concentration on an α-AlOOH surface that was coated with 0.1*M* H_3PO_4 (as in Fig. 4(a)) should have been 0.6–6 P atoms per square nanometer, which would correspond to bulk powder concentrations in the range of 0.3%–3% phosphorus.

IV. Discussion

The results of our surface-area and AFM experiments clearly demonstrate that phosphorus inhibits sintering and surface-area loss in α-Al_2O_3 powders that have been derived from α-AlOOH. However, even optimally doped powders sintered significantly, as the surface area was reduced from 150 m^2/g just after decomposition (400°C) to only 36 m^2/g after 24 h at 1000°C. The majority (>100 m^2/g) of this loss can be attributed to the elimination of pores within individual pseudomorphs, i.e., intra-pseudomorph sintering. This attribution is supported by the expectation that powders comprised of fully dense pseudomorphs would have surface areas of only 48 m^2/g, even in the absence of inter-pseudomorph sintering. Furthermore, within 10 h at 1000°C, cracks had healed over areas of >1 μm^2 on both undoped and phosphorus-doped pseudomorph surfaces that had been derived from single crystals (Fig. 4). Hence, it is unlikely that nanometer-scale pores could have persisted up to 24 h at 1000°C in pseudomorphs that were derived from α-AlOOH powder with an average particle size of <100 nm. The idea that the pores are eliminated at 1000°C is also supported by the fact that the surface areas of comparably doped products were virtually insensitive to the α-AlOOH decomposition temperature (400° or 500°C) and, therefore, the initial α-Al_2O_3 surface area (150 or 80 m^2/g). For example, undoped and magnesium- and iron-doped products that

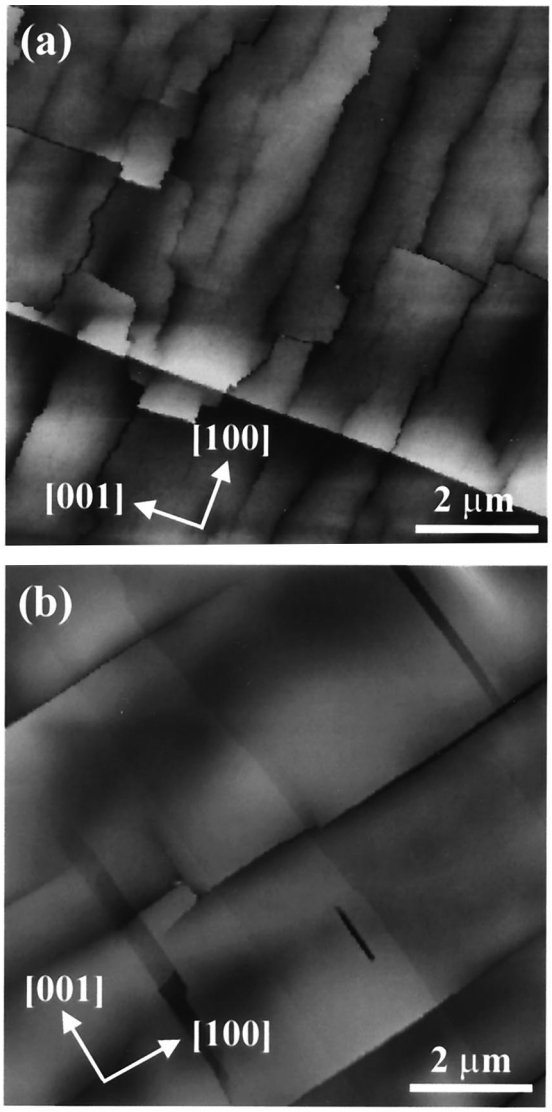

Fig. 4. Topographic AFM images of (a) phosphorus-doped and (b) undoped α-Al_2O_3 pseudomorph surfaces derived from α-AlOOH(010) after 12 h at 400°C and then 10 h at 1000°C. The black-to-white contrast in the images corresponds to 60 nm. The crystallographic directions are shown with respect to the parent α-AlOOH crystals.

were decomposed at 400° and 500°C all evolved to have surface areas of ~11 m^2/g after 24 h at 1000°C. This convergence indicates that the final surface area was determined by pseudomorph size, which was constant and fixed by the α-AlOOH particle size, and the extent of inter-pseudomorph sintering, rather than the pore structure of the pseudomorphs.

Considering the microstructure of the α-Al_2O_3 pseudomorphs, one would certainly expect intra-pseudomorph sintering to proceed rapidly, compared with inter-pseudomorph sintering. Because of the topotactic nature of the decomposition reaction, α-Al_2O_3 particles within a pseudomorph are ideally in the same crystallographic orientation.[15,16,32] Consequently, the formation and growth of interparticle necks will not, as a rule, require the creation of new grain-boundary area. At the most, some low-angle boundaries might be formed, although our AFM studies have shown that areas much larger than the α-AlOOH powder particle size were free of boundaries. Conversely, adjacent α-Al_2O_3 particles at pseudomorph–pseudomorph contacts will, in general, be arbitrarily oriented with respect to each other, necessitating that new high-angle boundaries be formed. Thus, the driving force for transport at pseudomorph–pseudomorph contacts should be less than that within a pseudomorph. Because of the large surface-area losses at 1000°C, inter-pseudomorph sintering must also have occurred, but the presence of phosphorus seems to have inhibited this process substantially. Hence, it should be possible to stabilize higher surface areas in phosphorus-modified α-Al_2O_3 by simply starting with finer α-AlOOH powder.

The effect of phosphorus doping on inter-pseudomorph sintering can be assessed within a framework analogous to scaling laws.[34–37] Because the α-Al_2O_3 powders were all derived from the same α-AlOOH, inter-pseudomorph sintering began with geometrically identical systems (i.e., ~48 m^2/g powder comprised of dense pseudomorphs) that likely progressed in geometrically identical manners, only at different rates. Hence, it was largely the interfacial and transport characteristics of the doped and undoped powders that might have differed. For geometrically identical systems that sinter via the same diffusive transport mechanism, the time required to achieve a certain microstructural change (for example in surface area) in one system (t_1) relative to that in a second (t_2) at fixed temperature can be expressed as follows:

$$\frac{t_1}{t_2} = \frac{(D\gamma\delta)_2}{(D\gamma\delta)_1}$$

where D_i, δ_i, and γ_i are the respective diffusion coefficient, diffusion width, and specific surface energy of system *i*. For the case of lattice diffusion, the δ_i would be dropped from the equation. Because the vapor pressure of Al_2O_3 is negligible at the temperatures studied, we will not consider the case of evaporation–condensation.[23] The effect of phosphorus on the quantity $D\gamma\delta$ can be assessed by comparing the times required to achieve comparable surface areas in pure and phosphorus-doped powders. For example, at least 100 h at 1000°C were required to attain a surface area of 30 m^2/g in phosphorus-doped α-Al_2O_3, but $<<1$ h was necessary in undoped samples. Assuming these conservative values, the presence of phosphorus reduced the quantity $D\gamma\delta$ to 1% of its intrinsic value at 1000°C. Although this is a rough approximation, it likely represents an upper limit, because the times selected were conservative and the surface area of undoped α-Al_2O_3 was reduced to 33 m^2/g within 1 h at only 700°C.

Data regarding the effect of magnesium, phosphorus, and iron doping on the surface energy of α-Al_2O_3 at 1000°C are not readily available. However, a qualitative assessment of the influence of the dopants on the surface energy can be made based on the surface energies of the corresponding liquid oxides at their melting points. Estimates of the surface energy for liquid alumina (Al_2O_3), magnesia (MgO), and iron(II) oxide (FeO) all are in the 0.55–0.66 J/m^2 range.[38] Surface energies in the solid state at 1000°C should be appreciably higher. The surface energy of phosphorus oxide (P_2O_5), which is a liquid at 1000°C, is ~0.05 J/m^2, which is an order of magnitude less than the other oxide melts and as little as 2% of that of solid α-Al_2O_3 ($\gamma \approx 2.5$ J/m^2).[19,38] Hence, magnesium and iron adsorption should have only a minor effect on the surface energy of α-Al_2O_3, whereas phosphorus adsorption could reduce it substantially, although certainly not by the two orders of magnitude that would minimally be needed to explain the sintering behavior.

To discuss the effect of phosphorus on the kinetic aspects of the sintering process, notably *D* and δ, the controlling transport mechanism must be identified. Considering the low temperatures investigated and the negligible vapor pressure of Al_2O_3 at these temperatures,[23] surface diffusion is the most likely candidate. Prior studies have concluded that surface diffusion controls the initial stage of sintering in much-coarser α-Al_2O_3 powders up to 1100°C.[36,39] Furthermore, recent time-dependent measurements of grain-boundary groove profiles in α-Al_2O_3 were consistent with surface-diffusion-controlled grooving at even 1400°C.[40] Assuming that the presence of magnesium and iron did not appreciably modify the surface energy of α-Al_2O_3, as argued earlier, it seems that their presence also did not have a significant effect on the transport kinetics at 1000°C, at least on a time scale of 24 h. Because it is unlikely that phosphorus could have reduced the surface energy of α-Al_2O_3 by a factor of >10, it must have also reduced the value of *D* and/or δ. Such a reduction could be accomplished through a variety of mechanisms, on which we can

only speculate at this time. One reasonable possibility is that the presence of phosphorus increases the activation energy for surface diffusion (Q), which might be expected, because of the covalent nature of the P—O bond. Because D is dependent exponentially on Q, only a modest (~10%) increase in Q would be needed to decrease D by a factor of 10, assuming an intrinsic value of 250 kJ/mol in α-Al_2O_3.[41]

V. Summary

Specific surface area measurements and atomic force microscopy (AFM) were used to investigate the influence of surface additions of magnesium, phosphorus, and iron on the low-temperature (≤1000°C) sintering of nanocrystalline α-Al_2O_3 that was derived from α-AlOOH. Synthetic α-AlOOH powder with a surface area of 50 m^2/g yielded α-Al_2O_3 products with surface areas of 150 and 80 m^2/g on dehydration at 400° and 500°C, respectively. Subsequent anneals at higher temperatures resulted in substantial reductions in surface area, and the powder products coarsened to 15 m^2/g within only 1 h at 1000°C. Magnesium and iron additions of 0.1%–5% had no detectable effect on this surface-area loss. Phosphorus doping, on the other hand, inhibited surface-area loss significantly, and α-Al_2O_3 samples that were doped with 1%–2% phosphorus had surface areas of >31 m^2/g after 100 h at 1000°C. AFM observations of α-Al_2O_3 pseudomorphs derived from α-AlOOH single crystals also demonstrated the inhibiting effect of phosphorus, as the cracks that formed during dehydration were eliminated at a reduced rate on phosphorus-doped surfaces. Using a scaling model, it was deduced that phosphorus doping reduced the product $D\gamma\delta$ (where D is the surface diffusivity, γ the surface energy, and δ the width) to <1% of its intrinsic value in α-Al_2O_3 at 1000°C, probably by reducing both the surface energy and surface diffusivity.

Acknowledgments

The authors gratefully acknowledge the National Museum of Natural History of the Smithsonian Institution (Washington, DC) for providing the single-crystal α-AlOOH samples and the use of the shared experimental facilities of the Materials Research Science and Engineering Center (MRSEC) at the Massachusetts Institute of Technology (supported by the National Science Foundation).

References

[1]W. H. Gitzen, *Alumina as a Ceramic Material*. American Ceramic Society, Columbus, OH, 1970.

[2]K. Wefers and C. Misra, "Oxides and Hydroxides of Aluminum," Alcoa Technical Paper No. 19, Alcoa Laboratories, Pittsburgh, PA, 1987.

[3]I. Levin and D. Brandon, "Metastable Alumina Polymorphs: Crystal Structures and Transition Sequences," *J. Am. Ceram. Soc.*, **81** [8] 1995–2012 (1998).

[4]H. C. Stumpf, A. S. Russell, J. W. Newsome, and C. M. Tucker, "Thermal Transformation of Aluminas and Alumina Hydrates," *Ind. Eng. Chem.*, **42** [7] 1398–403 (1950).

[5]A. S. Russell and C. N. Cochran, "Surface Areas of Heated Alumina Hydrates," *Ind. Eng. Chem.*, **42** [7] 1336–40 (1950).

[6]D. L. Trimm, *Design of Industrial Catalysts*; Ch. 5. Elsevier, Amsterdam, The Netherlands, 1980.

[7]P. Burtin, J. P. Brunelle, M. Pijolat, and M. Soustelle, "Influence of Surface Area and Additives on the Thermal Stability of Transition Alumina Supports, I: Kinetic Data," *Appl. Catal.*, **34**, 225–38 (1987).

[8]L. L. Murrell and N. C. Dispenziere Jr., "Silica-Stabilized Aluminas Resistant to Vanadium Attack under Sever High-Temperature Conditions," *J. Catal.*, **111**, 450–52 (1988).

[9]F. Oudet, P. Courtine, and A. Vejux, "Thermal Stabilization of Transition Alumina by Structural Coherence with $LnAlO_3$ (Ln = La, Pr, Nd)," *J. Catal.*, **114**, 112–20 (1988).

[10]M. F. L. Johnson, "Surface Area Stability of Aluminas," *J. Catal.*, **123**, 245–59 (1990).

[11]J. S. Church, N. W. Cant, and D. L. Trimm, "Stabilization of Aluminas by Rare Earth and Alkaline Earth Ions," *Appl. Catal. A*, **101**, 105–16 (1993).

[12]M. Inoue, H Otsu, H. Komonami, T. Nakamura, and T. Inui, "Thermal Stability of Phosphorus-Modified Alumina Prepared by the Glycothermal Method," *J. Mater. Sci. Lett.*, **13**, 787–89 (1994).

[13]Z. Weng-Sieh, R. Gronsky, and A. T. Bell, "Effects of Support Interactions on the Phase Stability of Rh Oxides Formed during the Aging of α-Alumina Supported Rh in Air," *J. Catal.*, **174**, 22–33 (1998).

[14]J. Reardon, A. K. Datye, and A. G. Sault, "Tailoring Alumina Surface Chemistry for Efficient Use of Supported MoS_2," *J. Catal.*, **173**, 145–56 (1998).

[15]G. Ervin Jr., "Structural Interpretation of the Diaspore–Corundum and Boehmite–γ-Al_2O_3 Transitions," *Acta Crystallogr.*, **5**, 103–108 (1952).

[16]J. Lima-de-Faria, "Dehydration of Goethite and Diaspore," *Z. Kristall.*, **119**, 176–203 (1963).

[17]A. H. Carim, G. S. Rohrer, N. R. Dando, S.-Y. Tzeng, C. L. Rohrer, and A. J. Perrotta, "Conversion of Diaspore to Corundum: A New α-Alumina Transformation Sequence," *J. Am. Ceram. Soc.*, **80** [10] 2677–80 (1997).

[18]J. M. McHale, A. Navrotsky, and A. J. Perrotta, "Effects of Increased Surface Area and Chemisorbed H_2O on the Relative Stability of Nanocrystalline γ-Al_2O_3 and α-Al_2O_3," *J. Phys. Chem. B*, **101**, 603–13 (1997).

[19]J. M. McHale, A. Auroux, A. J. Perrotta, and A. Navrotsky, "Surface Energies and Thermodynamic Phase Stability in Nanocrystalline Aluminas," *Science*, **277**, 788–91 (1997).

[20]R. L. Smith, G. S. Rohrer, and A. J. Perrotta, "Influence of Diaspore Seeding and Chloride Concentration on the Transformation of Diasporic Precursors to Corundum," *J. Am. Ceram. Soc.*, **84** [8] 1896–902 (2001).

[21]R. N. Das, A. Bandyopadhyay, and S. Bose, "Nanocrystalline α-Al_2O_3 Using Sucrose," *J. Am. Ceram. Soc.*, **84** [10] 2412–23 (2001).

[22]R. K. Pati, J. C. Ray, and P. Pramanik, "Synthesis of Nanocrystalline α-Alumina Powder Using Triethanolamine," *J. Am. Ceram. Soc.*, **84** [12] 2849–52 (2001).

[23]R. B. Bagwell and G. L. Messing, "Effect of Seeding and Water Vapor on the Nucleation and Growth of α-Al_2O_3 from γ-Al_2O_3," *J. Am. Ceram. Soc.*, **82** [4] 825–32 (1999).

[24]M. Pijolat, M. Dauzat, and M. Soustelle, "Influence of Additives and Water Vapor on the Transformation of Transition Aluminas into Alpha-Alumina," *Thermochim. Acta*, **122**, 71–77 (1987).

[25]Z. Hrabe, S. Komarneni, L. Pach, and R. Roy, "The Influence of Water Vapor on Thermal Transformations of Boehmite," *J. Mater. Res.*, **7** [2] 444–49 (1992).

[26]A. J. Perrotta; unpublished results.

[27]W. J. Smothers and H. J. Reynolds, "Sintering and Grain Growth of Alumina," *J. Am. Ceram. Soc.*, **37** [12] 588–95 (1954).

[28]K. A. Berry and M. P. Harmer, "Effect of MgO Solute on Microstructure Development in Al_2O_3," *J. Am. Ceram. Soc.*, **69** [2] 143–49 (1986).

[29]Y.-M. Chiang, D. Birnie III, and W. D. Kingery, *Physical Ceramics: Principles for Ceramic Science and Engineering*; pp. 372–88, 413–21. Wiley, New York, 1997.

[30]G. C. Bye and G. T. Simpkin, "Influence of Cr and Fe on Formation of α-Al_2O_3 from γ-Al_2O_3," *J. Am. Ceram. Soc.*, **57** [8] 367–71 (1974).

[31]R. L. Smith and G. S. Rohrer, "The Structure Sensitivity of H_xMoO_3 Precipitation on MoO_3(010) during Reactions with Methanol," *J. Catal.*, **184**, 49–58 (1999).

[32]F. Watari, P. Delavignette, and S. Amelinckx, "Electron Microscopic Study of Dehydration Transformations, II. The Formation of 'Superstructures' on the Dehydration of Goethite and Diaspore," *J. Solid-State Chem.*, **29**, 417–27 (1979).

[33]F. Watari, J. Van-Landuyt, P. Delavignette, S. Amelinckx, and N. Igata, "X-ray Peak Broadening as a Result of Twin Formation in Some Oxides Derived by Dehydration," *Phys. Status Solidi A*, **73**, 215–24 (1982).

[34]C. Herring, "Effect of Change of Scale on Sintering Phenomena," *J. Appl. Phys.*, **21**, 301 (1950).

[35]S. Prochazka and R. L. Coble, "Surface Diffusion in the Initial Sintering of Alumina Part I, Model Considerations," *Phys. Sintering*, **2** [1] 1–18 (1970).

[36]S. Prochazka and R. L. Coble, "Surface Diffusion in the Initial Sintering of Alumina, Part III, Kinetic Study," *Phys. Sintering*, **2** [2] 15–34 (1970).

[37]M. N. Rahaman, *Ceramic Processing and Sintering*. Marcel Dekker, New York, 1995.

[38]N. Eustathopoulos, M. G. Nicholas, and B. Drevet, *Wettability at High-Temperatures*; pp. 165–72. Pergamon/Elsevier, Oxford, U.K., 1999.

[39]J. M. Dynys, R. L. Coble, W. S. Coblenz, and R. M. Cannon, "Mechanism of Atom Transport During Initial Stage Sintering of Al_2O_3"; pp. 404–17 in Materials Science Research, Vol. 13, *Sintering Processes*. Edited by G. C. Kuczynski. Plenum Press, New York, 1980.

[40]D. Saylor and G. S. Rohrer, "Measuring the Influence of Grain-Boundary Misorientation on Thermal Groove Geometry in Ceramic Polycrystals," *J. Am. Ceram. Soc.*, **82** [6] 1529–35 (1999).

[41]J. M. Dynys, "Sintering Mechanisms and Surface Diffusion for Aluminum Oxide"; Ph.D. Thesis. Massachusetts Institute of Technology, Cambridge, MA, 1982. □